Excitation of vortices using linear and nonlinear magnetostatic waves

A. D. Boardman,[1,*] Yu. G. Rapoport,[2,†] V. V. Grimalsky,[3] B. A. Ivanov,[4] S. V. Koshevaya,[5] L. Velasco,[1] and C. E. Zaspel[6]
[1]*Joule Physics Laboratory, University of Salford, Salford, Greater Manchester, M5 4WT, United Kingdom*
[2]*Physical Faculty, Kiev Taras Shevchenko National University, prospect Glushkov 6, 03680 Kiev, Ukraine*
[3]*National Institute for Astrophysics, Optics, and Electronics, Puebla 72000, Puebla, Mexico*
[4]*Institute of Magnetism, National Academy of Science and Ministry of Education of Ukraine, 36-B Vernadskii Avenue, 03142 Kiev, Ukraine*
[5]*CIICAp, Faculty of Chemistry, Autonomous University of Morelos (UAEM), Av. Universidad, 1001, Z.P. 62210, Cuernavaca, Morelos, Mexico*
[6]*University of Montana–Western, Dillon, Montana 59725, USA*
(Received 2 August 2004; published 24 February 2005)

It is shown that stationary vortex structures can be excited in a ferrite film, in the important centimeter and millimeter wavelength ranges. It is shown that both linear and nonlinear structures can be excited using a three-beam interaction created with circular antennas. These give rise to a special phase distribution created by linear and nonlinear mixing. An interesting set of three clockwise rotating vortices joined by one counter-rotating one presents itself in the linear regime: a scenario that is only qualitatively changed by the onset of nonlinearity. It is pointed out that control of the vortex structure, through parametric coupling, based upon a microwave resonator, is possible and that there are many interesting possibilities for applications.

DOI: 10.1103/PhysRevE.71.026614 PACS number(s): 41.20.Jb, 42.25.Bs, 78.20.Bh

I. INTRODUCTION

The recognition that vortices are rather important manifestations of optical phase singularities has opened up a new frontier in optics. These "swirling" entities can, in principle, be used to carry data and point to a new era for communications. While electromagnetic vortices are attractive for modern optical applications, it should be noted that vortices, in general, are a common phenomenon and have been observed in both water and the atmosphere for hundreds of years. They are a common occurrence in plasma and atmospheric science, and striking examples include the behavior of Rossby [1] and Alfvén waves [2]. Even so, it is only in recent times that the wave field structure has been understood properly, from an electromagnetic point of view, and the full generic mathematical properties have been developed. Experimentally, vortices in liquids [3], space plasmas [4], and the atmosphere [5] have been thoroughly investigated but it is the recent studies, especially in nonlinear optics, that have stimulated an almost explosive development, in both theoretical and experimental contributions [6,7]. This work builds upon the pioneering work of Nye and Berry [8].

The successes of optical vortex theory and experiment have an importance that goes far beyond the boundaries of high frequency optics because the generic ideas ought to be applicable to magnetostatic waves and should impact upon quasioptical microwave and millimeter-wave systems. The latter are of increasing importance in surveillance utilizations, so any work in this area is likely to generate many applications. Up to now, however, no arrangements have been designed to excite vortices in the microwave or millimeter frequency range, even though the creation of a "vortex antenna" in the microwave and millimeter-wave ranges would be very important.

This paper addresses how this important step can be taken, by investigating phase singularities in forward volume magnetostatic waves (FVMSW's) [9]. The starting point is the famous Nye and Berry [8] definition, which states that a phase singularity in space occurs where the real and imaginary parts of the wave field vanish simultaneously, i.e., for a scalar wave field, represented by the complex function F, a phase singularity occurs whenever

$$F_r = 0, \quad F_i = 0. \tag{1a}$$

Here F_r and F_i are the real and imaginary parts, respectively, and the phase Φ is defined through

$$\tan(\Phi) = \frac{F_i}{F_r}. \tag{1b}$$

Obviously, Φ is indeterminate, whenever Eq. (1a) is satisfied; hence the term "singularity." Actually, this singularity may be associated with either an edge or a screw dislocation and it is the latter that characterizes vortices, which will be addressed here. The presence of a vortex means that the line integral of the spatial gradient of the phase, taken around the vortex center, or line, is some multiple of π, i.e.,

$$\oint (\vec{\nabla}\Phi) dl = 2n\pi, \tag{2a}$$

in which $n = 1, 2, \ldots$ is a positive integer, proportional to what has become known as the "topological charge." If $n = 0$ then a dipole vortex structure is said to exist.

The Poynting vector for the magnetostatic waves used in this paper is [10]

*Email address: a.d.boardman@salford.ac.uk
†Email address: laser@i.kiev.ua

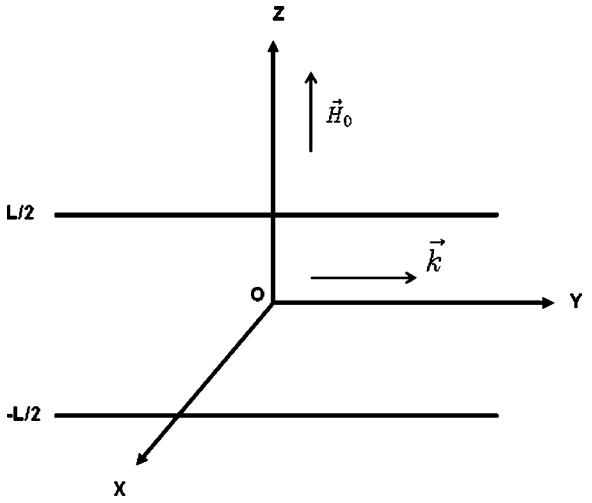

FIG. 1. Forward volume magnetostatic wave propagating in normally magnetized ferrite film. L is the width of the film, $\mathbf{k}$ is the wave number, and $\mathbf{H}_0$ is the applied magnetic field.

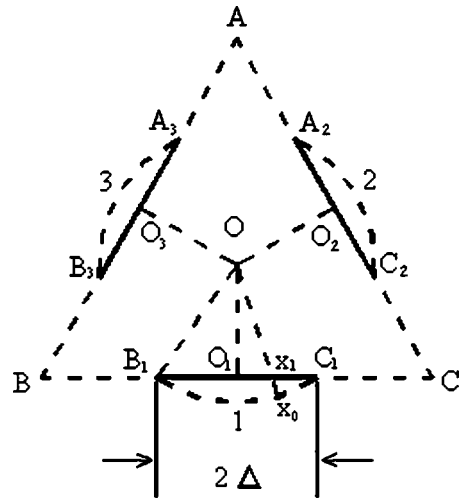

FIG. 2. Excitation of three waves by plane antennas (solid line sections $B_1O_1C_1$, $A_2O_2C_2$, and $A_3O_3B_3$), or by arc antennas (arcs B_1C_1, A_2C_2, and A_3B_3 of a circle around O shown as dashed lines; these arcs are not shown to scale for the convenience of displaying the geometrical calculations). Circular antennas are placed at $2\pi/3$ intervals around the center at O.

$$\vec{P} = \frac{c}{8\pi}\mathrm{Re}\left(\varphi\frac{\partial\vec{b}^*}{\partial t}\right) \tag{2b}$$

where φ and $\vec{b}$ are the magnetostatic potential and the magnetic induction, respectively. If a singularity like a vortex is present then the Poynting vector rotates around the "vortex center," which is a point in the two-dimensional case and an axis in the three-dimensional case. The surface of constant phase associated with a screw dislocation is helicoidal, so that the Poynting vector, which is directed along the normal, spirals about the propagation direction.

In the magnetostatic regime of a ferrite material

$$\vec{h} = -\vec{\nabla}\varphi, \tag{2c}$$

where $\vec{h}$ is the magnetic field and there is a potential carried by a magnetostatic wave of the form

$$\{\varphi = |\varphi|\exp[i\Phi] \tag{2d}$$

where Φ is the phase and the amplitude is φ.

The scalar function φ and h_Z, the component of the magnetic field normal to the surface of the ferrite film, sketched in Fig. 1, both satisfy conditions (1) and (2), for $n \neq 0$. On the other hand, the tangential components of the magnetic field h, lying in the OXY plane of the ferrite film, satisfy conditions (1) and (2) with $n=0$.

II. CIRCULAR ANTENNA EXCITATION OF LINEAR FORWARD VOLUME MAGNETOSTATIC WAVES

The geometry for forward volume magnetostatic waves and a sketch of the excitation arrangement are shown in Figs. 1 and 2. A linear FVMSW propagates in a ferrite film along the direction Y, normal to an applied magnetic field that is directed along the Z axis. The magnetostatic potential and field components are proportional to $\exp[i(\omega t)]$, where ω is the angular frequency. The field structure and dispersion relation are determined through the equation [9,10]

$$\mathrm{div}\vec{b} = [\mu(\varphi_{XX} + \varphi_{YY}) + \varphi_{ZZ}] = 0 \tag{3}$$

where

$$b_X = -(\mu\varphi_X - i\mu_a\varphi_Y), \quad b_Y = -(\mu\varphi_Y - i\mu_a\varphi_X), \quad b_Z = \varphi_Z \tag{4a}$$

inside the ferrite film, and

$$\mathrm{div}\vec{b} = -(\varphi_{XX} + \varphi_{YY} + \varphi_{ZZ}) \tag{4b}$$

outside the ferrite film. The quantities μ and μ_a are components of the permittivity tensor,

$$\mu = \frac{\omega_\perp^2 - \omega^2}{\omega_H^2 - \omega^2}, \quad \mu_a = \frac{\omega\omega_M}{\omega_H^2 - \omega^2}, \tag{4c}$$

in terms of the definitions $\omega_H \neq |\gamma|(H_0 - 4\pi M_0)$, $\omega_M \neq |\gamma|4\pi M_0$, and $\omega_\perp^2 = \omega_H(\omega_H + \omega_M)$, in which H_0 and $4\pi M_0$ are the bias externally applied magnetic field and the saturation magnetization of the ferrite film, respectively. γ is called the gyromagnetic ratio. The tangential components of magnetic field $\varphi_{X,Y}$ and the normal component of magnetic induction b_Z are continuous at the ferrite film boundaries. The latter are located at $Z = \pm L/2$, and the shape of the fundamental mode of the magnetostatic potential [9] is

$$\varphi = \left\{\begin{array}{ll} \dfrac{\cos(\sqrt{-\mu}|k|Z)}{\cos(\sqrt{-\mu}|k|L/2)}, & |Z| \leq L/2 \\ e^{-|k|Z}, & |Z| > L/2 \end{array}\right\} \times F(X,Y)e^{i\omega t}$$
$$\equiv f_z(z)F(X,Y)e^{i\omega t}, \tag{5a}$$

where k is determined from the dispersion equation

$$\tan(\sqrt{-\mu}kL/2) = \frac{1}{\sqrt{-\mu}}. \tag{5b}$$

Hence the equation for F is

$$\frac{\partial^2 F}{\partial X^2} + \frac{\partial^2 F}{\partial Y^2} + k^2 F = 0. \tag{5c}$$

For an excitation of a forward volume magnetostatic wave by the kind of circular antennas shown in Fig. 2, the solutions are complicated by the cylindrical geometry. In Fig. 2, circular antennae are placed at $2\pi/3$ intervals around the center at O. The distances from the center to the chords of these arcs are labeled OO_i $(i=1,2,3)$. The chords are segments of the triangle ABC. When excitation of the FVMSWs by arc antennas is considered, the geometrical optics is used to "transform or recalculate" the boundary conditions from the arcs to "effective straight line antennas" (see the end of Sec. III). The length of the section X_1X_0 is found as follows. $|O_1X_1|=x_1$, where x_1 is the coordinate of the point X_1 at the section O_1C_1. The radius of the arc B_1C_1 is $r=|OX_0|=|OB_1|$; $|OO_1|=\sqrt{r^2-\Delta^2}$; $|OX_1|=\sqrt{|OO_1|^2+|O_1X_1|^2}=\sqrt{|OO_1|^2+x_1^2}$ $=\sqrt{r^2-\Delta^2+x_1^2}$. Therefore

$$|X_1X_0| = |OX_0| - |OX_1| = r - \sqrt{r^2-\Delta^2+x_1^2} \approx \frac{\Delta^2 - x_1^2}{r}. \tag{6}$$

To be specific, only solutions with finite values of magnetostatic potential in the center of the circular antenna need to be considered. Hence, φ and $F(r,\theta)$ are finite, at $r=0$, where (r,θ) are cylindrical coordinates, with the origin coinciding with the center of the circular microstrip antenna. The Poynting vector in this system of coordinates has the components

$$P_r = -\frac{c}{8\pi}\mathrm{Re}\left[i\omega\varphi\left(i\mu_a \frac{1}{r}\frac{\partial\varphi^*}{\partial\theta} + \mu\frac{\partial\varphi^*}{\partial r}\right)\right],$$

$$P_\theta = -\frac{c}{8\pi}\mathrm{Re}\left[i\omega\varphi\left(-i\mu_a \frac{\partial\varphi^*}{\partial r} + \mu\frac{1}{r}\frac{\partial\varphi^*}{\partial\theta}\right)\right]. \tag{7}$$

If the radius of the microstrip antenna is r_0, then the magnetostatic potential is determined by the additional boundary condition

$$F(r_0,\theta) = Ce^{i\theta}, \tag{8}$$

where C is a real constant. The solution of Eq. (5c) is, therefore,

$$F(r,\theta) = Ce^{i\theta}\frac{J_1(kr)}{J_1(kr_0)}, \tag{9}$$

from which it is clear that $F(0,\theta)=0$ and a property associated with a vortex structure is guaranteed for FVMSWs excited by the circular antenna. Contour integration of the phase along a circular path around the phase defect at $r=0$ leads to $\oint_L d\Phi = \int_{0^+}^{2\pi} d\theta = 2\pi$, with the conclusion that $n=1$ and that the topological charge is 1. Although the field is determined by means of a single, scalar, magnetic potential function, it is also interesting to approach the investigation of the topological structure through the components of the magnetic field vector. The latter, for points on a circle of radius $r=\rho$, is

$$\begin{aligned}\vec{h}|_{Z=L/2} &= -\vec{\nabla}\varphi|_{Z=L/2} \\ &= \vec{e}_Z h_Z + \vec{e}_r h_r + \vec{e}_\varphi \vec{h}_\varphi \\ &= \vec{e}_Z kCe^{i\theta}\frac{J_1(k\rho)}{J_1(kr_0)} + \vec{e}_r kC^{i\theta}\frac{J_1'(k\rho)}{J_1(kr_0)} + \vec{e}_\theta \frac{1}{\rho}Ce^{i\theta}\frac{J_1(k\rho)}{J_1(kr_0)}\end{aligned} \tag{10}$$

where the common multiplier $e^{i\omega t}$ is omitted.

It is interesting that, although the real and imaginary parts of the field components h_Z, h_θ vanish at the center of the circle and lead to the same topological structure, the component h_r does not satisfy the condition of vanishing at the origin. Further confirmation of the presence of a vortex structure comes from the behavior of the Poynting vector, which rotates around the center. In fact, the only nonzero component of the Poynting vector is

$$P_\theta = \frac{c}{8\pi}|C|^2 I_z \frac{J_1(kr)}{J_0^2(kr_0)}\left[\frac{\mu}{r}J_1(kr) - \mu_a k J_1'(kr)\right], \tag{11}$$

where $I_z = \int_{-\infty}^{\infty} f_z^2(z)dz$, and $f_z(z)$ comes from Eq. (5a).

In summary, for field distributions associated with circular antenna structures with the kind of phase defects expected for vortex creation exist for the magnetostatic potential and the field components h_Z, h_θ, with a topological charge $n=1$, but for the field component h_r they exist for $n=0$.

From a practical point of view it is easier to use several short plane or arc antennas, placed along the corresponding circle, instead of deploying an entire circular antenna. In this paper two cases are developed, one consisting of three plane antennas and the other of three arc-shaped ones. All are located along the same circle and so the analysis rests upon a three-beam interaction. To simulate the phase distribution, a phase shift of $2\pi/3$ between the neighboring antennas will be used. The first case, addressed in the next section, is a simplified model of a three-linear-plane-wave interaction.

III. A LINEAR PHASE DEFECT STRUCTURE INDUCED BY THREE PLANE WAVES

The creation of a linear scalar vortex structure, through the interaction of three plane waves in a *bulk crystal*, has already been considered in the optical domain [11], but here a vector structure is considered using three forward volume magnetostatic waves in a ferrite thin film. As stated earlier, the directions of propagation of the three plane waves are displaced at angles $2\pi/3$ with respect to each other. In addition, they will also be assumed to have amplitudes $A_1=A_2=A_3=A$.

A phase defect of the magnetostatic potential φ is placed at the "center of interaction," which is the point O in Fig. 2. If it is assumed that the distances from all three antennas (shown as sections of solid lines $B_1O_1C_1$, $A_2O_2C_2$, and $A_3O_3C_3$ in Fig. 2) to the center at O are all equal, then $|O_1O|=|O_2O|=|O_3O|=r_0$. The initial phases of the potential at the antennas 1, 2, and 3 are Φ_1, Φ_2,and Φ_3, respectively.

Now consider the magnetostatic potential at points on the circle $r=\rho$ surrounding the center O, and set

$$k\rho \ll 1. \tag{12a}$$

Given that the polar axis is directed from point O, the center of the interaction, toward the center of the first antenna of Fig. 2, the potential at some point P with polar coordinates ρ, θ is

$$\varphi = Ae^{-ikr_0}e^{i\omega t}[e^{i\Phi_1}e^{ik\rho\cos\theta} + e^{i\Phi_2}e^{ik\rho\cos(\theta-2\pi/3)} + e^{i\Phi_3}e^{ik\rho\cos(\theta-4\pi/3)}]f_z(z). \tag{12b}$$

Putting $\Phi_1=0$, $\Phi_2=2\pi/3$, and $\Phi_3=4\pi/3$ the term in the square brackets of Eq. (12b) plays the role of an "effective complex envelope" $\tilde{A}$, where

$$\tilde{A} = e^{i\Phi_1}e^{ik\rho\cos\theta} + e^{i\Phi_2}e^{ik\rho\cos(\theta-2\pi/3)} + e^{i\Phi_3}e^{ik\rho\cos(\theta-4\pi/3)} = \tilde{A}' + i\tilde{A}'', \tag{13}$$

and, under the condition (12b),

$$\tilde{A}' \approx -(3/2)k\rho\sin\theta, \quad \tilde{A}'' \approx (3/2)k\rho\cos\theta, \tag{14a}$$

which leads to the equivalent representation

$$\tilde{A} = (3/2)k\rho e^{i(\theta+\pi/2)}, \quad \varphi = Ae^{-ikr_0}e^{i\omega t}\tilde{A}f_z(z). \tag{14b}$$

Obviously, the singularity condition (1a) is satisfied at the center of the circle. The phase Φ of complex amplitude $\tilde{A}$ is introduced through

$$\tan\Phi = \frac{\tilde{A}''}{\tilde{A}'}, \quad d\Phi = \frac{\tilde{A}'d\tilde{A}'' - \tilde{A}''d\tilde{A}'}{\tilde{A}'^2 + \tilde{A}''^2}. \tag{15}$$

If the point P is on the circle of radius ρ, then $d\Phi=d\theta$ and the phase gradient integral (2a) will yield the topological charge associated with a magnetostatic potential phase defect. Hence it is clear how a phase defect structure of a magnetostatic potential can be created. What is needed are three, equal-amplitude, interacting plane waves, moving under the angle restraint that they have normals that are inclined at $2\pi/3$ with respect to each other. Naturally this conclusion rests upon choosing appropriate initial amplitudes. It is straightforward to show that where $k\rho \ll 1$ the components of the Poynting vector are

$$P_r = 0, \quad P_\theta = \frac{c}{8\pi}I_z\frac{9}{4}|A|^2\omega k^2 r(\mu_a - \mu), \tag{16}$$

which demonstrates that the Poynting vector rotates around the center, as required for vortexlike structures to make their appearance. Some simulations to illustrate this case are shown in Fig. 3.

IV. ARC ANTENNA CREATION OF LINEAR AND NONLINEAR STRUCTURES WITH PHASE DEFECTS

The antenna structure is placed on the surface of the kind of normally magnetized ferrite film shown in the Fig. 1. As before, the structure consists of microstrip antennas generating three interacting stationary forward volume magnetostatic waves. This time, however, the antennas are the arcs of a circle that are labeled 1, 2 and 3 in Fig 2. The boundary conditions are transformed in this case to make effective antennas in the form of straight line segments $B_1O_1C_1$, $A_2O_2C_2$, and $A_3O_3C_3$ shown in Fig. 2. FVMSW beams interact principally in the region 4, but diffraction and possible nonlinearity change the simple geometrical optics picture of beam propagation. The interaction regions shown in Fig. 2 are shown to provide a simplified picture only. The interaction of three FVMSW beams in dimensionless form is modeled by the coupled equations

$$\frac{\partial U_j}{\partial y_j} + ig\frac{\partial^2 U_j}{dx_j^2} + iN\left(|U_j|^2 + 2\sum_{l\neq j}|U_l|^2\right)U_j + \gamma U_j = 0, \tag{17}$$

where $j,l=1,2,3$, U_j is the dimensionless complex amplitude of the magnetic potential, and N is a dimensionless nonlinear coefficient:

$$\varphi = 1/2U_{dj}f_z(Z)\exp[i(\omega t - ky_j)] + \text{c.c.}, \quad U_{dj} = U_jU_0 \tag{18a}$$

where U_{dj} are the true dimensional amplitudes of the jth beam and U_0 is an amplitude used for normalization. y_j is the direction of jth beam propagation in the corresponding coordinate (see Figs. 1 and 2), and $f_z(Z)$ is the transverse distribution function in the ferrite film [see also Eq. (5a)].

$$g = \frac{1}{2l_0k}, \quad N = N_d{U^2}_0l_0, \quad \gamma = \gamma_d l_0 \tag{18b}$$

are the respective dimensionless parameters of diffraction, self-interaction, and loss, in which $N_d=(\partial k/\partial|U_d|^2)_{\omega=\text{const}} = -1/V_g(\partial\omega/\partial|U_d|^2)_{k=\text{const}}$ and γ_d are the actual nonlinear coefficient and coefficient of loss, respectively. Typically,

$$l_0 = 1 \text{ cm}, \quad \gamma = 0.2, \quad N = 1, \tag{18c}$$

so these have been selected for the calculations reported here. In addition, the numerical simulations are based upon a ferrite film of thickness $L=10$ μm, and $|BC|a=1$ cm. The frequencies and wave numbers of each of the three interacting FWMSWs are identical and are set equal to $\omega\approx\omega_H \approx \omega_M \sim 3\times10^{10}s^{-1}$ and $k\approx150$ cm^{-1}. The nonlinear coefficient N_d for the exchange-free nonlinear Schrödinger envelope equation can be determined using expansion in series by small amplitudes of the nonlinear dispersion equation [12] or by means of bilinear relationships analogous to the energy conservation law [13]. Estimates show that for $N=1$, $l_0=1$ cm, the normalizing amplitude is such that $kU_0\sim2$ Oe, or $U_0\sim1.3\times10^{-2}$ Oe cm; the value of N_d can be found from the relation (18b) with a given N and l_0 [see also Eq. (18c)] and the estimated value of U_0.

The beams converge more toward the center of the interaction, taking into account some possible diffraction, through the bending of the antennas into arcs. The boundary conditions are introduced by transforming the conditions from the actual arc antennas into those that pertain to effective straight line antennas. As a result of this strategy, the following

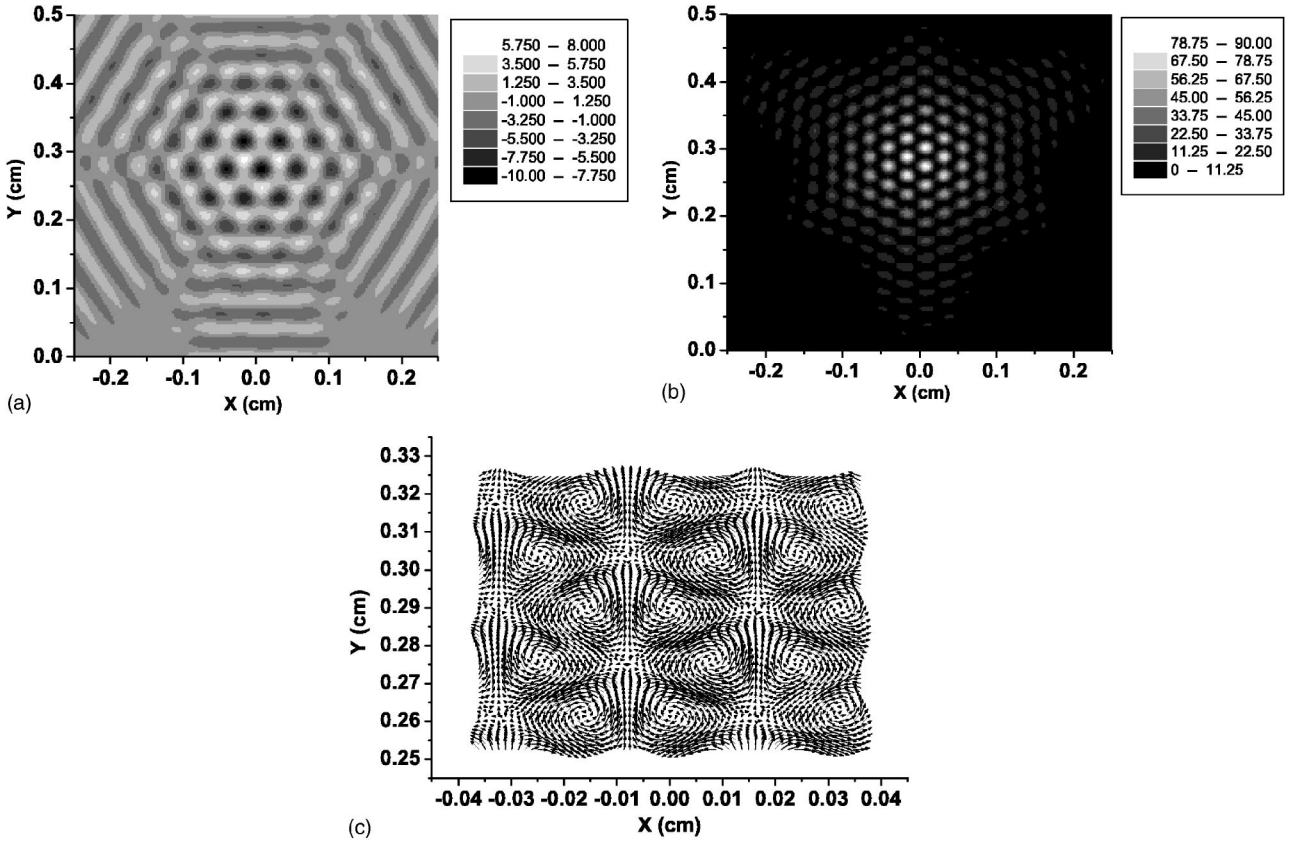

FIG. 3. Spatial vortex structure excited by three linear, equal-absolute-amplitude, unshifted ($x_{i0}=0$, $i=1,2,3$), unfocused magnetostatic plane wave beams. The X and Y axes lie along the directions of the lines O_1C and O_1O in Fig. 2, respectively. The origin of the coordinates coincides with the point O_1 (center of the antenna of the first MSW beam) in Fig. 2. The same applies to Figs. 4–13 below; the beam width is $x_0=0.1$ and remains at this value for the computations displayed in this paper. (a) spatial distribution of Re $\varphi(x,y)$, the real part of the magnetostatic potential; (b) distribution of $|\varphi(x,y)|^2$; (c) display of a vector that is proportional to the Poynting vector.

analogous boundary conditions are used for beams $i=1,2,3$, using the first one as a reference beam:

$$U_i(x_i,y_i) = U_{i0}\exp\{-[(x_i - x_{i0})/x_0]^2\}\exp[i\Phi_i + i\psi(x_i)]. \tag{19}$$

Here U_{i0} is the maximum amplitude of the ith beam, the initial phases Φ_i are determined by the relationships defined earlier, all the beam widths are x_0, x_{i0} are the positions of the beam centers relative to the central points of the antennas and the phases $\psi(x_i)$ arise because of the transformation from arcs to the corresponding straight segments, e.g., for beam 1, the transition is from arc 1 to the straight segment B_1C_1, which is illustrated in Fig. 2 for the case when $x_{i0}=0$. Hereafter beams with $x_{i0}=0$ and $x_{i0}\neq 0$ are called "unshifted" and "shifted" beams, respectively. To find the phases $\psi(x_i)$, consider, for the sake of definiteness, the beam in Fig. 2, for which $|B_1C_1|=2\Delta \ll r=a\sqrt{3}/6$, where the radius of the circle is $r=|OB_1|$ and Δ is equal approximately to half the length of the FVMSW antenna. An application of simple ray optics and using Eq. (6) then leads to the result (see also the caption to Fig. 2)

$$\psi(x_1) = -ik|X_1X_0| = r - \sqrt{r^2 - \Delta^2 + x_1^2} \approx \frac{\Delta^2 - x_1^2}{r}. \tag{20}$$

V. SPATIAL PATTERNS OF EXCITED LINEAR STRUCTURES

Setting $N=0$ yields linear structures and these are shown in Figs. 3–5. These cover the following cases: (a) no focusing or shifting of the beam for which $\exp[i\psi(x_i)]=1$ and $x_{i0}=0$; (b) focusing without shifting of the beam, for which $\exp[i\psi(x_i)]\neq 1$ and $x_{i0}=0$; (c) $\exp[i\psi(x_i)]\neq 1$ and $x_{i0}\neq 0$, which means that there is both focusing and beam shifting. Note also that Figs. 3–5 correspond to the interaction of three magnetostatic waves with equal absolute amplitude values. Figures 3(a), 4(a), and 5(a), Figs. 3(b), 4(b), and 5(b), and Figs. 3(c), 4(c), and 5(c), respectively, show the spatial distributions of Re $\varphi(x,y)$, $|\varphi(x,y)|^2$, and a vector proportional to the Poynting vector. If required the coefficient of proportionality can be determined in each particular case and has only been selected from the point of view of clarity and quality of presentation of the essential features. $h_z \sim \partial\varphi/\partial z \sim F(x,y)\,\partial f_z(z)/\partial z$, Re $\varphi(x,y)$, and $|\varphi(x,y)|^2$ have the following physical interpretations. To within an accuracy of some multiplier, they are Re $\varphi(x.z)|_{z=L/2} \sim$ Re $F(x,y) \sim h_z|_{z=L/2}$, $|\varphi(x,z)|^2_{z=L/2} \sim |h_z|^2_{z=L/2}$. Without focusing (see Fig. 3), in the vicinity of the center, a magnetostatic wave beam, with a finite width equal to x_0, is approximately a plane wave. It can be seen from Figs. 3(a) and 3(b) that, as a result

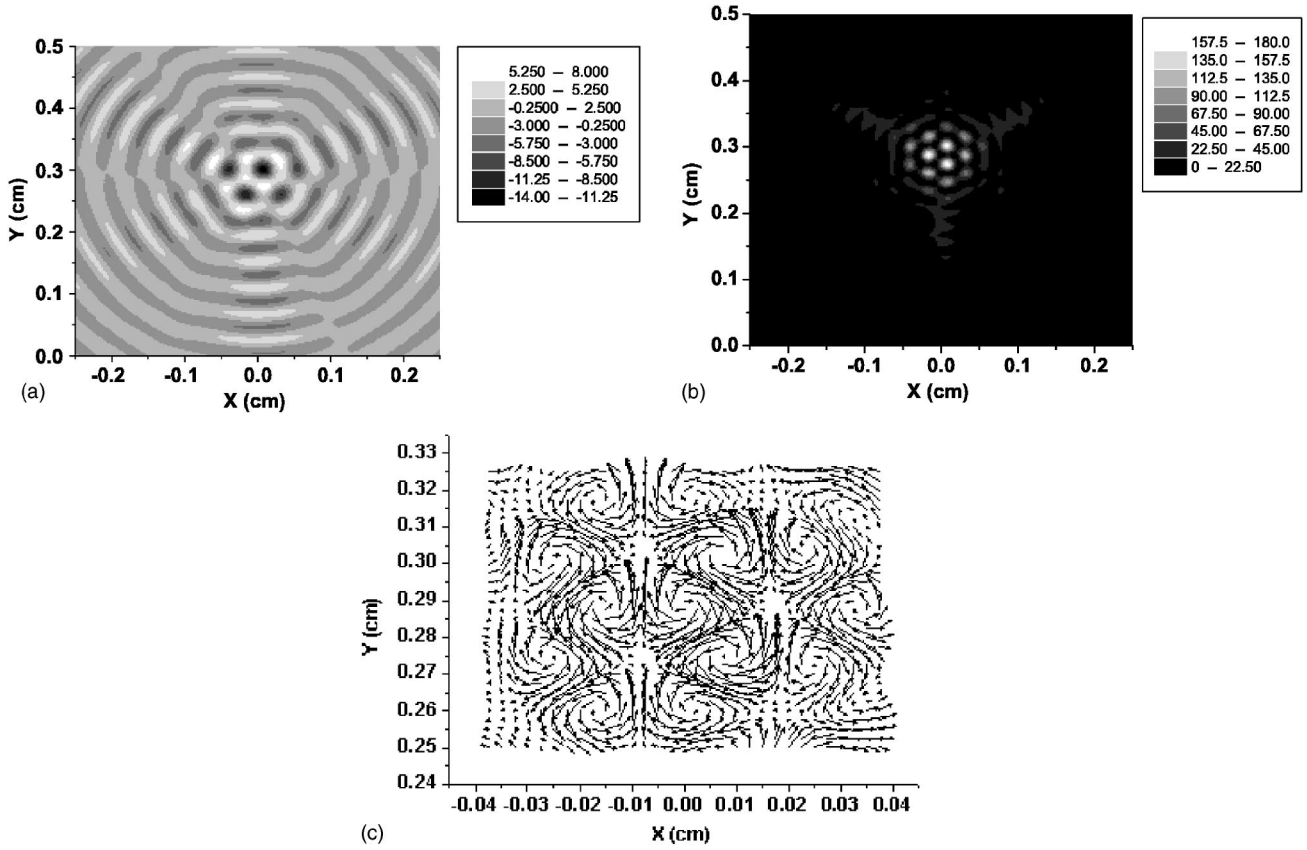

FIG. 4. Spatial vortex structure excited by three linear, equal-amplitude, unshifted, focused beams. (a) Spatial distribution of Re $\varphi(x,y)$; (b) $|\varphi(x,y)|^2$; (c) vector proportional to the Poynting vector.

of a linear interaction among the three waves, a structure with a quasiperiodic set of singular points is generated. Figures 4(a) and 4(b) show clearly the effect of focusing in the central region of the three beams excited by arc antennas. In this case, *singular* quasiperiodic structures for Re $\varphi(x,y)$ and $|\varphi(x,y)|^2$ are also generated in the central region of the ferrite film. Quasiperiodic structures for Re $\varphi(x,y)$ and $|\varphi(x,y)|^2$ are absent, however, when the three focused beams have centers displaced, with respect to the center of the interaction, i.e., $x_{i0} \neq 0$, as can be appreciated from Figs. 5(a) and 5(b). Quasiperiodic vortex structures around O with (dimensionless) coordinates $x=0$, $y=0.287$ or (dimensional) $x=0$, $y=a/(2\sqrt{3})$ for undisplaced beams are shown in Figs. 3(c) (no focusing) and 4(c) (focusing). The formation of a system of vortices, with right and left directions of rotation of the Poynting vector, is obvious from these figures. The value of the magnetostatic potential φ was found at O by a direct numerical calculation. It is zero in both the linear (Figs. 3–5) and the nonlinear cases, when the absolute values of the amplitudes of all three interacting waves are equal to each other.

In the case of three beams with shifted centers ($x_{i0} \neq 0$) a symmetrical structure of right- and left-rotating vortices is formed around O as seen in Fig. 5(c). In the linear case, for equal amplitudes of the interacting beams, the unit value of topological charge was obtained by direct numerical computation. In the general nonlinear wave case, however, a geometrical method is more convenient. For both focusing and nonlinear beams, direct computation of the phase integral is not very accurate because the accuracy is restricted by the value $k\sqrt{dx^2+dy^2}$, which is of the order of 0.15. Even though this is an adequate limitation for the calculation of the potential envelope function, within the usual slowly varying approximation, the inaccuracy of the phase integral is rather large. An effective alternative to direct computation of this integral, however, is to build a graph of the phase along some circumference. Taking into account that each jump of phase is equal to π, the number of jumps in the phase along this circumference then yields a value of topological charge. Figure 6(a) shows the spatial distribution of the phase in the vicinity of the origin for linearly interacting focusing beams with equal absolute values of the amplitude. Two phase jumps, each approximately equal to π, can be clearly seen, so that the topological vortex charge of the corresponding vortex is equal to 1. Figure 6(b) shows the same phase distribution, but over a larger part of the interaction region.

Note that the motion of the magnetostatic potential in the vicinity of the center can be described as a rotation. There is a localization of the magnetostatic potential along the Z direction (in the region of the film) which is described by the function included in the relationship (5a). The magnetostatic potential inside the ferrite film is the result of interference of two waves counterpropagating and forming a standing wave in the Z direction. The phase defects for nonfocused and focused interacting beams, respectively, can be called arrangements of quasiscrew phase dislocations or a set of quasiscrew vortices in a ferrite film. The term quasiscrew is

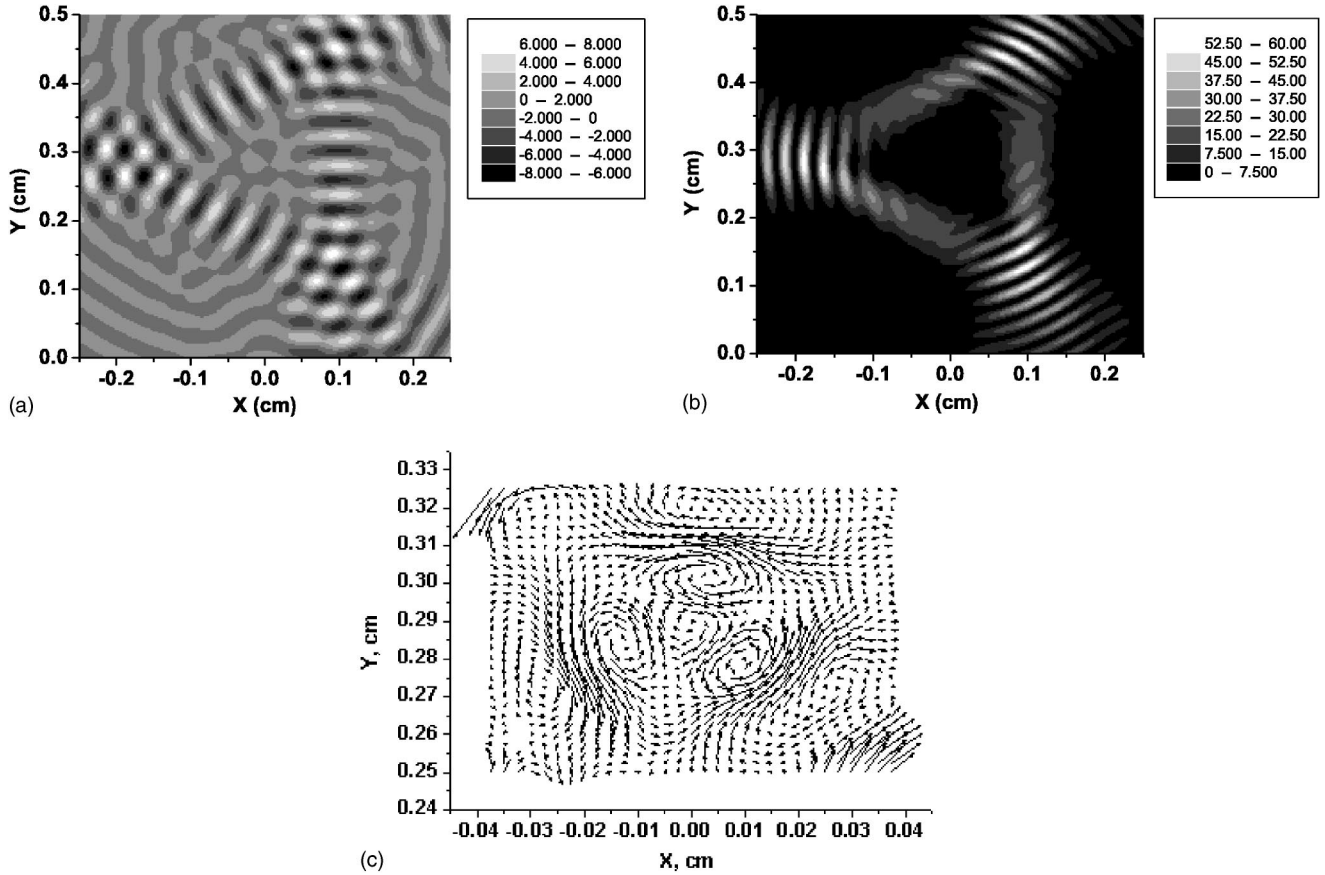

FIG. 5. Spatial vortex structure excited by three linear, equal-amplitude, shifted ($x_{i0}=0$, $i=1,2,3$), focused beams. (a) Spatial distribution of Re $\varphi(x,y)$; (b) $|\varphi(x,y)|^2$; (c) Poynting vector distribution.

meant to convey the fact that a real screw is replaced in the ferrite film by a rotation. If three linear (optical) plane waves in an unbounded medium have wave vectors in the same plane, and equal amplitudes, wave numbers, and frequencies, a periodic set of screw dislocations occurs. The symmetry of the wave structure with a set of phase defects that are vortices is interesting. For the geometry depicted in Fig. 2, using three waves with equal amplitudes, wave numbers, and frequencies and initial phases equal to $\Phi_1=0$, $\Phi_2=2\pi/3$, and $\Phi_3=4\pi/3$, the total magnetostatic potential satisfies the following relationship:

$$\varphi(\theta_0+2\pi/3)=\varphi(\theta_0)e^{i2\pi/3}, \tag{21a}$$

where θ_0 is the polar angle and the relationship describes the macroscopic symmetry of the structure considered. In distinction to this, circular symmetry is evident only in the neighborhood of the vortex axis. For three identical interacting, lossless, linear plane waves with equal amplitudes the analysis works well within the vicinity of any phase defect. If loss, diffraction, nonlinearity, or focusing is present, the amplitude of each of the waves will depend on the coordinates, and Eq. (14a) will be valid only for the vicinity of the geometrical center of the structure. In the latter case, in the other points of the phase defects shown in Figs. 3(a), 3(b), 4(a), and 4(b), Eq. (14a) will be valid only approximately, because the supposition that all the wave amplitudes are equal to each other will not be true in the vicinity of other phase defect points. At the same time, because the amplitudes of the waves change slowly in time and space it can be said, at least for the phase defects seen in Figs. 3(a), 3(b), 4(a), and 4(b), that being in the neighborhood of the center gives them validity. Therefore, even for lossy and dispersive [Figs. 3(a) and 3(b)], focused [Figs. 4(a) and 4(b)], or nonlinear (see Figs. 8 and 9 below) beams, the structures can be treated as a set of quasiscrew dislocations. As can be seen from Eq. (14a), and also from the way that the phase is determined [see Eqs. (1b) and (15)]

$$\Phi(\theta+\pi)=\Phi(\theta). \tag{21b}$$

Figure 7 shows a small fragment of the phase distribution with equal phase contours, for three focused linear beams with equal amplitudes [Figs. 6(a) and 6(b)] in the close vicinity of the central point and demonstrates the above phase periodicity. Note that Fig. 7 is a small fragment of Fig. 6 so it reflects the same structural symmetry as Fig. 6. Equation (21b) characterizes the microscopic symmetry of the structure in the neighborhood of the phase defect point(s) while Eq. (21a) characterizes the macroscopic symmetry of the structure as a whole, relative to the geometrical center.

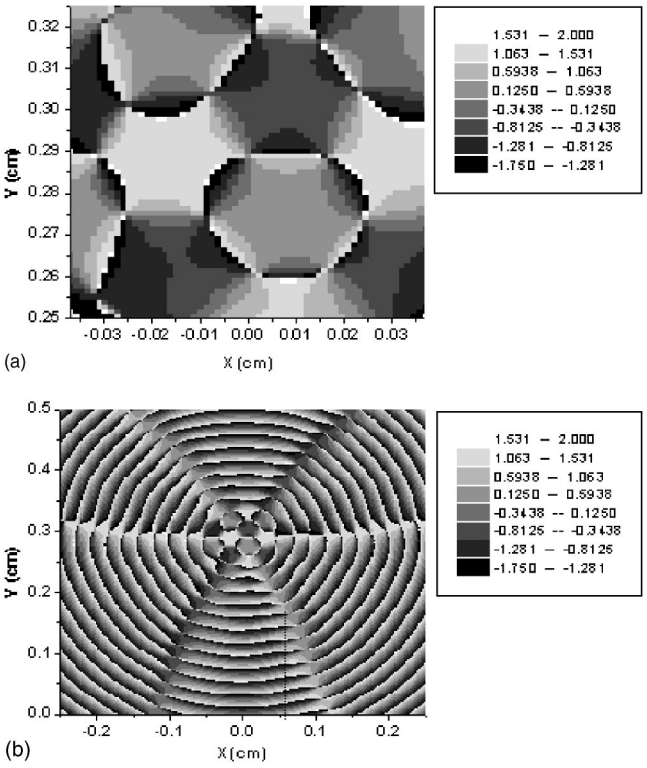

FIG. 6. (a) Spatial distribution of the magnetostatic potential phase Φ in the neighborhood of the center point O, for three equal-amplitude, linear, focused beams. (b) Spatial distribution of magnetostatic potential Φ for the same parameters as in (a), but in wider spatial region.

VI. INFLUENCE OF NONLINEARITY, UNEQUAL BEAM AMPLITUDES, AND SHIFTED BEAM CENTERS

For a linear three-wave magnetostatic interaction, defined with a suitable relative phase shift, a rotating vortex structure has been established in the previous sections. The influence of nonlinearity upon the shape of this structure and also the vortex charge will now be addressed, together with a study of the role of interacting beam asymmetry, when the moduli of their amplitudes are unequal. The work described here can be put into a broader context by noting that, in [14] (devoted to nonlinear singular optics), in particular, three-wave interaction was considered and the possibility of vortex charge redistribution was discussed.

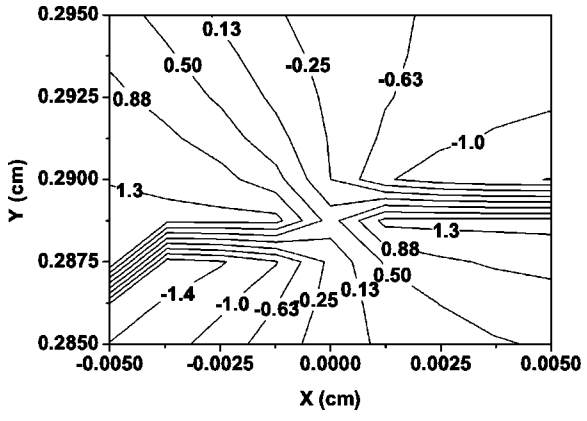

FIG. 7. Contour map fragment of spatial distribution (shown in Fig. 6) of magnetostatic potential phase Φ in the close vicinity of the point O, the geometrical center of the structure (shown in Fig. 2). The values of Φ in radians on the lines of the constant phase are shown by the numbers inside the figure.

Suppose, for simplicity, that only the first two polar modes are excited, i.e., $F_{12}(r,\theta)=A_1(r)e^{i\theta}+A_2(r)e^{2i\theta}$, where the values $A_{1,2}$ are real and $F_{12}(0,\theta)=0$. F_{12} is a function describing qualitatively a vortex structure, with the center at $r=0$. The outcomes of a direct calculation, of the integral of the phase gradient are 2π, 3π, and 4π, respectively, for $A_2=0$, $A_1=A_2$, and $A_1=0$. A more general result can be easily obtained using $F_{12}(r,\theta)=A_1(r)F_1(\theta)F_2(r,\theta)$, where $F_1(\theta)=e^{i\theta}$, $F_2(r,\theta)=1+r_0(r)e^{i\theta}$, and $r_0(r)=A_2(r)/A_1(r)$. A simple geometrical argument is enough to investigate the phase integrals for $r_0<1$, $r_0=1$, and $r_0>1$.

The corresponding vortex charges are 1, 3/2, and 2 in these cases, so that if the ratio of the amplitudes of the second and main polar harmonics can be changed (linearly or nonlinearly), the vortex charge can also be changed. The transformations of topological charge during free space propagation of a light wave, which is a combination of a Gaussian beam with a multiply charged optical vortex within a Gaussian envelope, were studied in [15]. In addition, it interesting to observe that the possibility of generating an optical vortex with a fractional charge after the diffraction of a linear optical beam on a thin binary amplitude grating has already been discussed [16].

In the present calculations, only rather low levels of harmonics are excited, and they determine the nonlinear coefficient needed for the envelope equation. The nonlinearity provides self- and cross interactions of the main harmonic amplitudes, in the vicinity of the singular points. The higher harmonics are included only implicitly into the system of coupled envelope equations through the nonlinear coefficient because the amplitudes of the harmonics are much smaller than the amplitudes of the three main interacting beams. A small enough nonlinearity will not influence the charge of the generated vortex. The numerical calculations presented below confirm this conclusion.

Figures 8–13 are generated for dimensionless magnetic

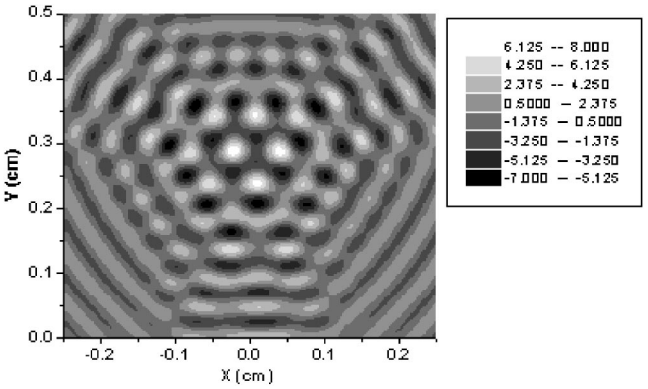

FIG. 8. Nonlinear structure Re $\varphi(x,y)$ for the same parameters as in Fig. 3(a). Dimensionless input beam amplitudes $U_{10}=U_{20}=U_{30}=3$.

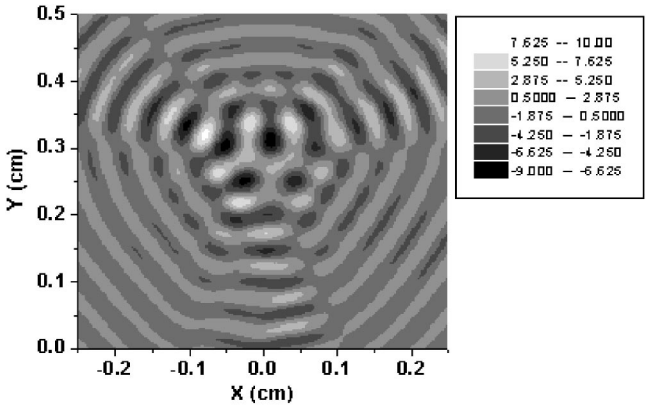

FIG. 9. Nonlinear structure Re $\varphi(x,y)$ for the same parameters as in Fig. 4(a). Dimensionless input beam amplitudes $U_{10}=U_{20}=U_{30}=2.95$.

field amplitudes $U_j \sim 2$–3; values that are necessary to provide the nonlinear effects described below. Note that further increase of the input amplitudes may lead to a second-order spin-wave instability [17–19]. The possibility of exciting exchange spin waves (with the same frequency as the incident beams) is not taken into account in the present paper and will be the subject of future work. The nonlinear calculations presented here show a qualitative influence of nonlinearity on vortex formation due to the three-beam interaction. The influence of the nonlinearity upon the shape of the spatial structures can be seen in Figs. 8 and 9, which are computed with equal absolute values of all nonlinear beam amplitudes. They show what happens for cases in which there is absence or presence of focusing. Comparing Figs. 8 and 9 with Figs. 3(a) and 4(a) shows that the nonlinearity leads to nonlinear two-dimensional diffraction. This causes broadening of the region of interaction and this is accentuated for focused beams, as can be appreciated by looking at Figs. 4(a) and 9. The difference between the linear and nonlinear structures in the absence of focusing is rather less than in the presence of focusing. Simultaneous asymmetry of the interacting beams brings out the most pronounced effect of the nonlinearity. As can be seen from Figs. 4(c) and 5(c), equal-amplitude linear

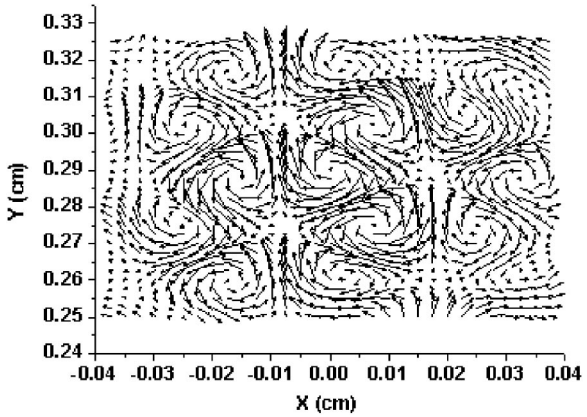

FIG. 10. Spatial distribution of field of the Poynting vector excited by three unshifted, non-equal-amplitude, linear, focused beams. Input beam amplitudes are $U_{10}=U_{20}=2.5$, $U_{30}=2.0$.

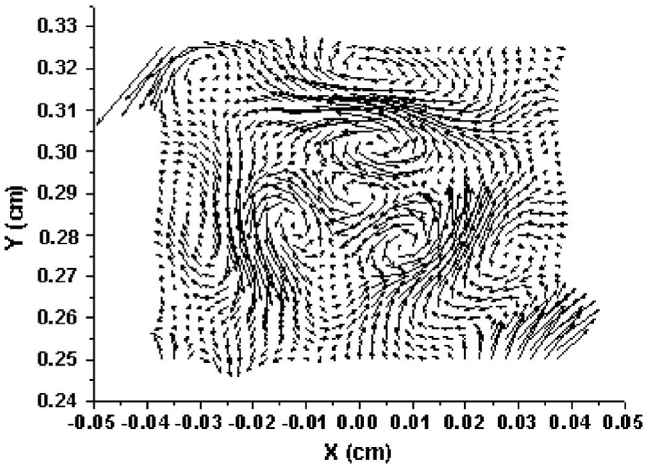

FIG. 11. Spatial distribution of field of the Poynting vector excited by three shifted, non-equal-amplitude, linear, focused beams. Absolute values of input beam amplitudes are $U_{10}=U_{20}=2.5$, $U_{30}=2$.

focused beams lead to a system of right- and left-rotating vortices that are symmetrical, regardless of whether they are shifted or not. If the linear beams have only slightly different absolute amplitudes, almost symmetric vortex structures are maintained and are shown in Figs. 10 and 11. Switching on the nonlinearity, for the amplitude values used in the linear structures, changes the situation to that shown in Figs. 12 and 13. Here it can be seen that the vortex structure formed by unshifted beams, endowed with different absolute amplitudes, shifts only slightly, as a whole, due to nonlinearity. If the beam centers are shifted then nonlinearity causes a rather complicated rebuilding of the vortex structure topology, as seen by comparing Figs. 5(c) and 11 with Fig. 13. Figure 13 reveals that the nonlinearity causes a rotation of the structure as a whole, spatial shifting of the points with phase defects, and a rebuilding that includes merging with a neighboring part of the structure. Overall, the conclusion is that in the absence of nonlinearity, slightly different amplitudes for the interacting beams permit the symmetry to remain but nonlinearity causes it to disappear. Note that it is also probably

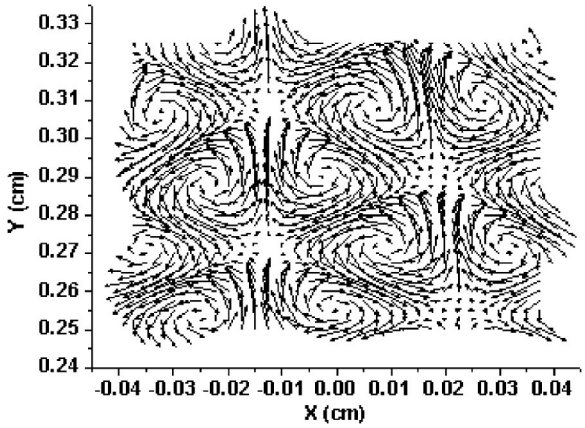

FIG. 12. Distribution of Poynting vector for the same parameters as in Fig. 10 but now with a nonlinear interaction of the magnetostatic beams.

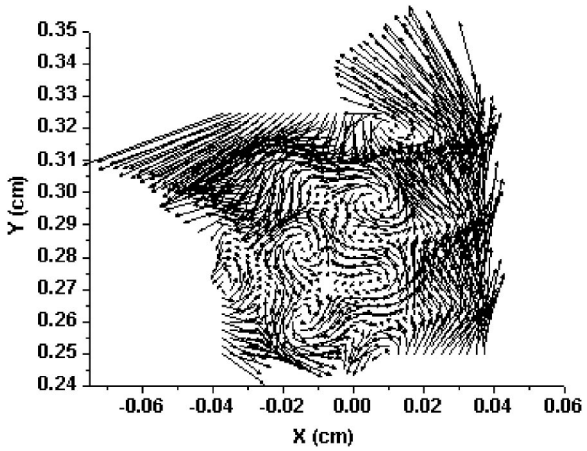

FIG. 13. Distribution of Poynting vector for the same parameters as in Fig. 11, taking into account a nonlinear interaction of the beams.

possible to create vortices using structures containing layers with higher nonlinearity than pure yttrium iron garnet (YIG) films possess, e.g., ferrite-paraelectric structures [20,21].

Using just visual evidence, presented in the form of the Poynting vector and phase spatial distributions, no points have been discovered where, simultaneously, the complex amplitude of the magnetostatic potential is zero and the phase integral around this point is different from 2π. In other words, for the linear or nonlinear interaction of three magnetostatic beams, under the condition that there is only an insignificant presence of higher harmonics, the vortex charge does not differ from 1 or -1.

VII. DISCUSSION AND CONCLUSIONS

It has been shown that some stationary vortex structures can be excited experimentally in a ferrite film. One suggestion is that the vortex structure can be exposed by a Brillouin scattering method [22]. These vortex structures are in the technically important centimeter and millimeter ranges. YIG or hexaferrite material may be used, but without using superconductivity or an exchange interaction. The main requirement for an experimental arrangement would be to maintain the necessary difference of phases between the antennas exciting the three interacting beams. In the future, nonstationary structures and the combination of vortex excitation with parametric interaction will be considered.

On the basis of the present work, linear and nonlinear vortex structures can be excited in a ferrite film, using a three-beam interaction with a $2\pi/3$ phase difference between the second and first and the third and second beams. If the centers of the beams are not displaced then Figs. 3(c), 4(c), 10, and 12 show what can happen to focused and nonfocused beams. Quasiperiodic structures are formed with vortex singularities and topological charge equal to 1 or -1. If focused beams, with displaced centers, interact with each other then a system of three clockwise-rotating vortices with one counter clockwise-rotating vortex in the center can be formed, as shown in Figs. 5(c) and 11.

If the absolute values of the beam amplitudes are equal then the main effect of the nonlinear diffraction is to broaden the interacting structures. For focused beams, a broadening of the region of interaction around the central point also occurs. If the moduli of the amplitudes of interacting beams with shifted centers are different, nonlinearity causes shifting and a rotation of the structure as a whole. A vortex exists in the linear case, surrounded by three symmetrical vortices. A vortex structure of three beams with different absolute values of the input amplitudes changes qualitatively due to nonlinearity. At the same time, no nonlinear change of vortex charge is obtained under the condition of a small level of higher harmonics adopted in the present modeling.

One direction for future investigation is to search for a nonlinear change in the vortex charge using layered structures that include materials with higher nonlinear coefficients such as ferrite-paraelectric-dielectric materials, or just paraelectric waveguides, where dispersion is smaller and nonlinearity larger than in ferrites. As a result, the effective generation of higher harmonics can be expected, and, therefore, a nonlinear vortex charge change. Another interesting possibility is the generation of vortex structures using an amplitude-dependent group velocity, which leads to the propagation of different parts of a pulse, with different velocities and phase defect structure formation [14]. To do this, structures with large nonlinearity and large enough dispersion are necessary. Probably, paraelectric-ferrite structures [20] combining the high dispersion of ferrite films and large paraelectric nonlinearity [21] would be suitable for this. The control of vortex structure characteristics could be achieved using two counterpropagating pulses that are in antiphase and including a relative shifting of their centers, together with parametric coupling between them. This kind of parametric coupling could be provided using a microwave resonator [23]. There are indeed a lot of interesting possibilities for centimeter and millimeter range vortex research based upon multilayered structures that include ferrite films.

[1] V. I. Petviashvili, JETP Lett. **32**, 619 (1980).
[2] P. K. Shukla, Phys. Scr. **32**, 141 (1985).
[3] N. Kukharkin and S. A. Orszag, Phys. Rev. E **54**, R4524 (1996).
[4] V. M. Chmyrev, S. V. Bilichenko, O. A. Pokhotelov, V. A. Marchenko, V. I. Lazarev, A. V. Streltsov, and L. Stenflo, Phys. Scr. **38**, 841 (1988).
[5] V. A. Andryshenko, Izv. Acad. Sci. USSR, Mech. Liq. Gas **N2**, 186 (1978) (in Russian).
[6] B. Luther-Davis, J. Christou, V. Tikhonenko, and Yu. V. Kivshar, J. Opt. Soc. Am. B **14**, 3045 (1997).
[7] T. Kambe, T. Minota, and M. Takaoka, Phys. Rev. E **48**, 1866 (1993).
[8] J. F. Nye and M. V. Berry, Proc. R. Soc. London, Ser. A **336**,

165 (1974).
[9] R. W. Damon and J. R. Eshbach, J. Phys. Chem. Solids **19**, 308 (1961).
[10] A. I. Ahkiezer, V. G. Bar'yahtar, and G. Peletminskiy, *Spin Waves* (Nauka, Moscow, 1967).
[11] J. Masajada and B. Dubik, Opt. Commun. **198**, 21 (2001).
[12] A. K. Zvezdin and A. F. Popkov, JETP **84**, 606 (1983).
[13] V. V. Grimalsky, Yu. G. Rapoport, and A. N. Slavin, J. Phys. IV **7**, C1-393 (1997).
[14] M. S. Soskin and M. V. Vasnetsov, Pure Appl. Opt. **7**, 301 (1998).
[15] M. S. Soskin, V. N. Gorshkov, M. V. Vasnetsov, J. T. Malos, and N. R. Heckenberg, Phys. Rev. A **56**, 4064 (1997).
[16] I. V. Basistiy, M. S. Soskin, and M. V. Vasnetsov, Opt. Commun. **119**, 604 (1995).
[17] A. G. Gurevich and G. A. Melkov, *Magnetization Oscillations and Waves* (CRC Press, Boca Raton, FL, 1996).
[18] H. Suhl, J. Phys. Chem. Solids **1**, 209 (1957).
[19] Y. T. Zhang, C. E. Patton, and G. Srinivasan, J. Appl. Phys. **63**, 5433 (1988).
[20] V. Demidov, P. Edenhofer, and B. Kalinikos, Electron. Lett. **37**, 1154 (2001).
[21] V. V. Grimalsky and S. V. Koshevaya, Pis'ma Zh. Tekh. Fiz. **13**, 1070 (1987) (in Russian).
[22] A. V. Bagada, G. A. Melkov, A. A. Serga, and A. N. Slavin, Phys. Rev. Lett. **79**, 2137 (1997).
[23] M. Bauer, O. Buttner, S. O. Demokritov, B. Hillebrands, V. Grimalsky, Y. Rapoport, and A. N. Slavin, Phys. Rev. Lett. **81**, 3769 (1998).